Ultrasonics Sonochemistry 111 (2024) 107136

Contents lists available at ScienceDirect

Ultrasonics Sonochemistry

journal homepage: www.elsevier.com/locate/ultson

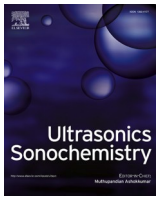

Ultrasound-assisted extraction of triterpenoids from *Chaenomeles speciosa* leaves: Process optimization, adsorptive enrichment, chemical profiling, and protection against ulcerative colitis

Mengyang Hou [a], Jingchun Shi [a], Chengyuan Lin [a], Lin Zhu [a,b,*], Zhaoxiang Bian [a,b,*]

[a] Centre for Chinese Herbal Medicine Drug Development, Hong Kong Baptist University, Hong Kong 999077, PR China
[b] School of Chinese Medicine, Hong Kong Baptist University, Hong Kong 999077, PR China

ARTICLE INFO

Keywords:
Chaenomeles speciosa leaves
Triterpenoids
Ultrasound-assisted extraction
Enrichment
UPLC-QTOF-MS/MS, HPLC-QQQ-MS, Ulcerative colitis

ABSTRACT

For the valorization of *Chaenomeles speciosa* leaves, this study focused on extraction, enrichment, chemical profiling, and investigation of the biological activity of its abundant triterpenoid components. Initially, the total triterpenoids in *C. speciosa* leaves were extracted by ultrasonic-assisted extraction (UAE) method, with the extraction process optimized through response surface methodology (RSM). Under the optimal conditions of extraction solvent 93 % EtOH, ultrasound power 390 W, extraction time 30 min, extraction temperature 70 °C, liquid-to-solid ratio 25 mL/g, and 2 extraction cycles, the maximum total triterpenoids yield (TTY) reached 36.77 ± 0.40 mg/g. The total triterpenoids in the crude extract were subsequently enriched by X-5 resin column chromatography, resulting in a fourfold increase in purity, reaching 73.27 ± 0.84 %. Thirteen compounds in the triterpenoid-rich fraction (TRF) were identified through UPLC–QTOF-MS/MS, and five major triterpenoids (oleanolic acid, ursolic acid, betulinic acid, maslinic acid, and pomolic acid) were simultaneously quantified by HPLC–QQQ-MS. Furthermore, TRF demonstrated a notable amelioration against dextran sodium sulfate (DSS)-induced ulcerative colitis in mice, indicating its promise as a potent intervention for this condition. In summary, this study will contribute to enhancing the utilization efficiency of *Chaenomeles speciosa* leaves.

1. Introduction

Chaenomeles speciosa is a perennial plant of the Rosaceae family, native to temperate regions of China, Japan, and Korea [1]. The fruit of *C. speciosa*, called "MuGua" in China, is renowned for its exceptional nutritional profile and potential health benefits. It has been extensively utilized as a raw material for producing a variety of food and beverage products, including marmalades, candied snacks, syrups, liquors, and juices [2]. In traditional Chinese medicine, MuGua is applied to alleviate a variety of conditions, including rheumatism, arthralgia, beriberi, indigestion, vomiting, diarrhea, hepatitis, and the common cold [3]. However, phytochemical studies have revealed that *C. speciosa* leaves contain a rich array of bioactive compounds, including triterpenoids, (poly)phenols, tocols, and amino acids [4,5]. *C. speciosa* leaves mainly contain pentacyclic triterpenoid compounds, which have been reported to possess various important pharmacological activities [6]. Consequently, considering the necessity for the comprehensive development of MuGua resources, further investigation of the leaves is warranted, especially regarding the triterpenoid constituents.

The extraction of active ingredients is a critical initial step in the field of natural product development, serving as an important portal for accessing and harnessing the potential therapeutic values of natural resources [7]. Traditional extraction methods for the recovery of triterpenoids, such as maceration, reflux, and Soxhlet extraction, typically require excessive solvents and extended processing times, potentially leading to the degradation of target compounds and reduced extraction yields [8]. In recent years, many innovative extraction techniques have emerged to surmount the constraints posed by traditional methods. Ultrasound-assisted extraction (UAE) stands out among these cutting-edge techniques because of its enhanced extraction efficiency, lower energy requirements, shorter extraction time, and ability to preserve the integrity of thermolabile compounds [9]. The improved efficiency of UAE in extracting bioactive components from plant matrices is largely attributed to the cavitation effect induced by ultrasonic waves, since the implosion of cavitation bubbles can destroy plant cell walls, increase solid–liquid contact, and promote solvent penetration, thereby

* Corresponding authors at: Centre for Chinese Herbal Medicine Drug Development, Hong Kong Baptist University, Hong Kong 999077, PR China (L. Zhu).
E-mail addresses: zhulin@hkbu.edu.hk (L. Zhu), bzxiang@hkbu.edu.hk (Z. Bian).

https://doi.org/10.1016/j.ultsonch.2024.107136
Received 2 September 2024; Received in revised form 12 October 2024; Accepted 28 October 2024
Available online 30 October 2024

increasing the extraction rate [10]. Furthermore, another essential step in drug development is enrichment, which is vital for ensuring the purity, efficacy, and safety of drug candidates. One of the most versatile and effective enrichment methods employed in the pharmaceutical industry is the use of macroporous adsorption resins. Resin-based enrichment offers several advantages, including high selectivity and adsorption capacity, improved recoveries, reduced processing time, and the ability to process large sample volumes, makeing it an ideal choice for enriching natural products and has been widely utilized [11]. The combined UAE and macroporous adsorption resin enrichment of triterpenoids have been widely studied [12,13].

Over the past decade, UPLC-QTOF-MS^n has become a formidable analytical strategy for the exhaustive profiling of plant metabolites [14]. UPLC efficiently separates compounds in complex plant extracts, with higher resolution and faster analysis time. The analytes are subsequently subjected to tandem mass spectrometry, which elucidates their structures through multiple fragmentation and mass determination steps. TOF mass analyzers offer outstanding mass accuracy for compound identification, with high mass resolution that distinguishes isomers [15]. These features are indispensable for the thorough characterization of intricate plant metabolites, including triterpenoids [16,17]. Furthermore, for quantitative analysis, triple quadrupole (QQQ) mass spectrometry represents an exceptional choice, offering versatile operational modes such as selected ion monitoring (SIM) and multiple reaction monitoring (MRM) for highly targeted analysis, providing superior sensitivity and selectivity for quantification of analytes even within complex matrices [18].

Inflammatory bowel disease (IBD), a condition that includes both Crohn's disease and ulcerative colitis, is characterized by enduring immune-mediated inflammation, disruption of intestinal homeostasis, and dysbiosis of the gut microbiome, resulting from a multifactorial interplay of environmental factors, genetic predisposition, and immune system dysregulation [19]. Conventional pharmacological interventions for IBD commonly rely on chemical drugs such as salicylazosulfapyridine and mesalazine, which can effectively relieve symptoms but are often accompanied by uncontrollable side effects [20]. Emerging evidence indicates that natural products, including triterpenoids, exhibit significant therapeutic potential for IBD in a dextran sulfate sodium (DSS)-induced ulcerative colitis mouse model [21,22].

With the purpose of fully harnessing the potential of *Chaenomeles speciosa* resources, the initial focus of this work was on the UAE of total triterpenoids from its leaves, with the extraction process optimized through response surface methodology (RSM) for maximum yield. Macroporous adsorption resin was then used to enrich the triterpenoids. The chemical profile of the triterpenoids-rich fraction (TRF) was characterized via UPLC–QTOF-MS/MS, and five major triterpenoid components were subsequently quantified via HPLC–QQQ-MS. Finally, the protection of TRF against dextran sulfate sodium (DSS)-induced ulcerative colitis in mice was evaluated.

2. Materials and methods

2.1. Chemicals and reagents

Oleanolic acid, betulinic acid, pomolic acid, and ursolic acid standards were procured from Yuanye Biotech Co., Ltd. (Shanghai, China). Maslinic acid standard and X-5 resin were procured from Macklin Biochemical Co., Ltd. (Shanghai, China). GR grade ethanol (EtOH) and LC–MS grade acetonitrile were procured from Duksan Pure Chemicals Co., Ltd. (Ansan, Korea). DSS was obtained from MP Biomedicals, Inc. (California, USA).

2.2. Plant material

Chaenomeles speciosa leaves were collected from Pingdingshan city, Henan Province, in August 2023. The leaves were then crushed, sieved through a 40-mesh screen, and stored in a digital dry cabinet for subsequent analysis.

2.3. Ultrasound-assisted extraction of total triterpenoids

2.3.1. Single-factor experimental design

In this work, the UAE of total triterpenoids from *C. speciosa* leaves was conducted by a KQ-500DE ultrasonic processor (40 kHz, Kunshan Ultrasonic Instruments Co., Ltd., Jiangsu, China). To determine the impact of various parameters on the total triterpenoids yield (TTY, Y), a single-factor experimental design was employed, the specifics of which are detailed in Table S1. Specifically, a range of six factors was investigated: the EtOH concentration (X_1, 45 %-95 %), ultrasonic power (X_2, 200–450 W), extraction time (X_3, 10–60 min), temperature (X_4, 20–70 °C), liquid–solid ratio (X_5, 10–35 mL/g), and number of extraction cycles (X_6, 1–4).

2.3.2. Response surface experimental design

Informed by the single-factor experimental results, the key parameters (X_1, X_2, X_3, and X_4) affecting Y and their respective ranges were identified, and a three-level four-variable Box–Behnken design (BBD) was performed. Table S2 lists the actual values of independent variables and their corresponding coding levels. The statistical relationship between the response variable and the independent variables was described by fitting the results of 29 randomly sequenced experiments into a polynomial model, the generalized form of which is presented below:

$$Y = \beta_0 + \sum_{i=1}^{k} \beta_i X_i + \sum_{i=1}^{k} \beta_{ii} X_i^2 + \sum_{i=1}^{k} \sum_{j=i+1}^{k-1} \beta_{ij} X_i X_j \quad (1)$$

where X_i and X_j denote the independent variables; β_0 represents the intercept; while β_i, β_{ii}, and β_{ij} signify the linear, quadratic, and interaction effects, respectively, with k being the count of independent variables.

2.4. Heat reflux extraction

The heat reflux extraction was conducted under optimized UAE conditions, which included the use of 93 % ethanol as the extraction solvent, an extraction time of 30 min, a temperature of 70 °C, a liquid-to-solid ratio of 25 mL/g, and two extraction cycles.

2.5. Enrichment of triterpenoids by macroporous resin adsorption chromatography

The extraction of triterpenoids from *C. speciosa* leaves (100 g) was performed according to the optimized UAE protocol. Subsequent to the centrifugation of the extract mixture, the supernatant was blended with pretreated X-5 resin (15 g). This mixture was concentrated at 50 °C under reduced pressure until the weight remained constant. The dried resin laden with the sample was subsequently placed into a column (φ = 32 mm) filled with X-5 resin. The elution program started with 6 bed volumes (BV, where 1 BV = 180 mL) of water, followed by 6 BV of 30 % EtOH and 6 BV of 60 % EtOH, and finally 6 BV of 90 % EtOH, all at a flow rate of 2 BV/h. The eluate, rich in triterpenoids, was collected, concentrated under reduced pressure, and then lyophilized, yielding a triterpenoids-rich fraction (TRF).

2.6. Measurement of total triterpenoid content

The total triterpenoid content was determined according to a previous report [23]. Briefly, a 100 μL aliquot of the sample mixture, prepared by dissolution in 5 % (w/v) vanillin-acetic acid, was mixed with 400 μL of perchloric acid. The blend was then heated at 60 °C for 15 min. After incubation, the mixture was rapidly cooled on ice. Subsequently,

50 μL of the mixture, along with 200 μL of acetic acid, was pipetted into 96-well plates. The absorbance at 545 nm was measured by a SpectraMax® iD5 microplate reader (Molecular Devices LLC, San Jose, CA, USA). An standard calibration curve ($y = 1.1555x + 0.0579$) was established using ursolic acid, where x and y represent the absorbance and concentration of ursolic acid, respectively, yielding an R^2 of 0.9996 over the range of 0.1–0.6 mg/mL.

2.7. UPLC–ESI-QTOF-MS/MS conditions

An Agilent 1290 Infinity II UPLC system was linked with an Agilent 6546 quadrupole time-of-flight mass spectrometer featuring a Dual AJS ESI source was used for qualitative analysis. The injection volume was designated as 1 μL, with the column temperature held constant at room temperature. Chromatographic separation was achieved using an Agilent ZORBAX Eclipse Plus C18 column (2.1 × 100 mm, 1.8 μm). Mobile phase A consisted of 0.1 % formic acid in water, and mobile phase B was acetonitrile. The elution of analytes occurred at 0.4 mL/min, following a gradient program of 0–10 min at 60–75 % B, 10–16 min at 75–95 % B, 16–17 min at 95–60 % B, and 17–20 min at 60 % B. Data acquisition for the Q-TOF mass spectrometer was conducted in auto MS/MS mode at a rate of 2 spectra/s. N_2 served as the drying gas at a nebulizer pressure of 45 psi and a flow rate of 8 L/min at 320 °C. The sheath gas temperature was 350 °C with a flow rate of 11 L/min, while the capillary and nozzle voltages were set at 3,500 V and 1,000 V, respectively. The secondary mass collision energy was set at 15 and 35 eV, and the MS and MS/MS scan range was from 50 to 1000 m/z in negative ion mode.

2.8. HPLC-QQQ-MS quantitative analysis

2.8.1. Analysis conditions

HPLC analysis was performed using an Agilent 1290 Infinity II system. The samples were chromatographed on an Alltima C18 column (250 mm × 4.6 mm, 5 μm). The sample injection volume was 2 μL, and the column temperature was set at 40 °C. The mobile phase consisted of 50 mM ammonium acetate in H_2O (phase A, adjusted to pH = 8 with ammonia) and methanol (phase B). The mobile phases were pumped at 0.6 mL/min using the following elution procedure: 0–12 min, 92 % B; 12–13 min, 92–100 % B; 13–14 min, 100–92 % B. An Agilent G6470B triple-quadrupole mass spectrometer was employed to generate the mass spectrometry data. The conditions for the negative ESI source were set as follows: the gas temperature was 350 °C with a flow rate of 10 L/min, the sheath gas temperature was also 350 °C with a slightly lower flow rate of 8 L/min, the nebulizer pressure was 45 psi, the capillary voltage was set at 3500 V, and the nozzle voltage was set at 1000 V. SIM parameters for the targeted triterpenoid compounds are presented in Table S3.

2.8.2. Method validation

The HPLC-QQQ-MS quantitative method was evaluated for linearity, linear range, limit of quantification (LOQ), limit of detection (LOD), precision, and recovery. The LOD and LOQ were assessed at signal-to-noise ratios of 3:1 and 10:1, respectively. Precision was determined by the relative standard deviation (RSD) of the intraday (samples analyzed six times on a single day) and interday (evaluated over six consecutive days) response signals. Recovery assays were performed with extracts from *C. speciosa* leaves that included the reference compounds.

2.9. Therapeutic effect of TRF in the DSS-induced colitis model

2.9.1. Modeling and drug treatment

Six-week-old male C57BL/6 mice were acclimated for one week and then divided into 6 groups ($n = 6$): the control, model, 5-ASA, TRF-L, TRF-M, and TRF-H groups. The control group was administered deionized water, whereas the remaining groups were treated with a 2 % DSS aqueous solution for six consecutive days to induce the disease model. The 5-ASA, TRF-L, TRF-M, and TRF-H groups were orally gavaged with mesalazine SR granules (600 mg/kg/d), TRF-L (100 mg/kg/d), TRF-M (200 mg/kg/d), or TRF-H (400 mg/kg/d) from days 0 to 9. The mice from all the groups fasted overnight and were sacrificed via cervical dislocation under anaesthesia on day 10.

2.9.2. Conventional efficacy indexes

The body weights of the mice were monitored daily during the entire experimental duration. The health status of the mice was evaluated by evaluating the disease activity index (DAI), which included scores for weight loss, stool consistency, and fecal bleeding according to our previous scoring criteria [24]. Furthermore, the colon lengths were compared between the groups, the spleen weights were measured, and the spleen index (spleen-to-body weight ratio) was calculated.

2.9.3. Histology

Colon tissues underwent fixation in 4 % paraformaldehyde for 24 h, followed by dehydration, paraffin embedding, sectioning into 4 μm slices, and subsequent staining with hematoxylin and eosin (H&E) for histological evaluation of the lesions. The severity of histological damage and inflammatory infiltration was scored in a blinded manner, and the scoring criteria were according to a previous report [25].

2.10. Statistical analysis

The data are presented as the mean ± standard deviations (SD) and were derived from at least three parallel replicates. Design Expert 13.0 software was used for response surface experimental design and subsequent data analysis. Statistical analysis was conducted via one-way or two-way ANOVA using GraphPad Prism 9.5.1. Significance levels are denoted as $^*p < 0.05$, $^{**}p < 0.01$, and $^{***}p < 0.001$, $^{****}p < 0.0001$.

3. Results and discussion

3.1. Analysis of single-factor experimental results

3.1.1. Effect of the EtOH concentration on the TTY

The influence of EtOH concentration on TTY is depicted in Fig. 1A, which shows an increase in TTY from 16.54 ± 0.64 to 32.77 ± 0.56 mg/g as the EtOH concentration rose from 45 % to 85 %. However, further increasing the EtOH concentration resulted in a decrease in TTY, a trend similar to that observed in the UAE of triterpenoids from *Jatropha curcas* leaves [8]. Owing to the hydrophobic nature of triterpenoids in *C. speciosa* leaves, higher EtOH concentrations facilitated triterpenoid extraction on the basis of the principle of similar compatibility. However, the higher EtOH concentration could lead to the dissolution of more liposoluble impurities, thereby impeding the extraction of triterpenoids. Therefore, the optimal extraction solvent was considered to be 85 % EtOH.

3.1.2. Effect of ultrasonic power on the TTY

The influence of ultrasonic power on the TTY is depicted in Fig. 1B. As the ultrasonic power increased from 200 to 350 W, the TTY increased from 25.76 ± 0.54 to 32.97 ± 0.50 mg/g. However, further increasing the ultrasonic power resulted in a decrease in TTY, a trend similar to that observed in the UAE of triterpenoids from loquat peel [12]. Within the 200–350 W range of ultrasonic power, TTY showed a positive correlation with increasing power levels. Higher power inputs resulted in more pronounced disruption of plant cell walls, facilitating better solvent penetration and diffusion into the plant matrix, which promoted the release and extraction of triterpenoid compounds. However, it is worth noting that ultrasonic power levels exceeding 350 W could potentially result in the degradation of triterpenoid molecules [26]. Thus, the optimal ultrasonic power was considered to be 350 W.

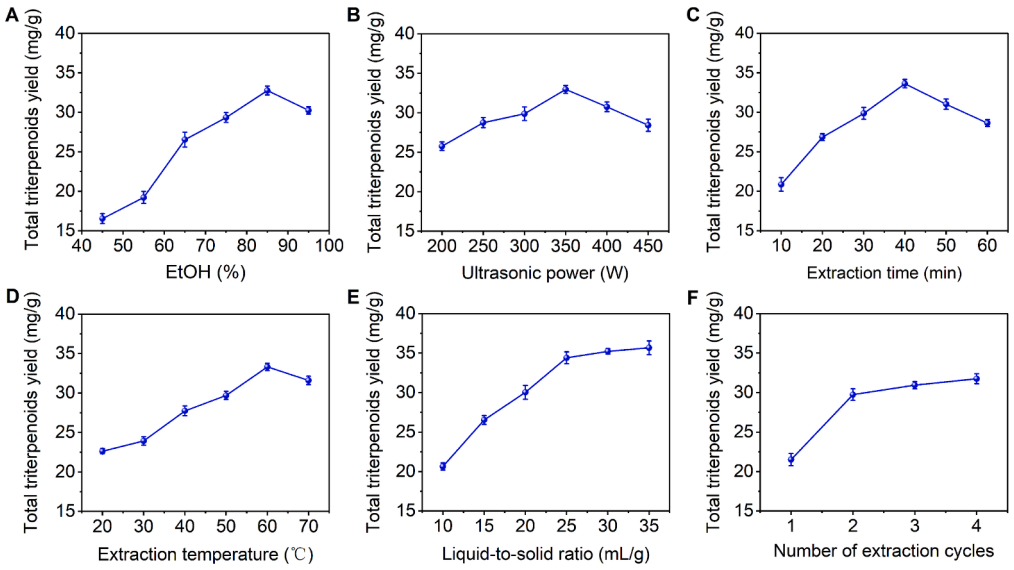

Fig. 1. Effects of independent variables on the TTY. (A) EtOH concentration; (B) ultrasonic power; (C) extraction time; (D) extraction temperature; (E) liquid-to-solid ratio; (F) number of extraction cycles.

3.1.3. Effect of extraction time on the TTY

The influence of extraction time on the TTY is illustrated in Fig. 1C. As the extraction time increased from 10 to 40 min, the TTY increased from 20.86 ± 0.85 to 33.63 ± 0.53 mg/g. However, further prolonging the extraction time led to a decrease in TTY, a pattern similar to that observed in the UAE of triterpenoids from *Hippophae rhamnoides* L. pomace [27]. The initial increase in TTY with increasing extraction time could be attributed to the increased solvent–solute interaction, which facilitated the release of more triterpenoid compounds from the plant matrix. However, excessively long extraction periods led to increased dissolved impurities and degradation of the target analytes, leading to the observed decrease in TTY at extended time points [28]. Thus, the optimal extraction time was considered to be 40 min.

3.1.4. Effect of extraction temperature on the TTY

The influence of the extraction temperature on the TTY is shown in Fig. 1D. As the extraction temperature increased from 30 to 60 °C, the TTY increased from 22.64 ± 0.33 to 33.32 ± 0.45 mg/g. However, exceeding 60 °C during the extraction process led to a decrease in TTY. A phenomenon akin to that also observed in the UAE of triterpenoids from *Boletus edulis* [29]. The initial increase in TTY with increasing temperature could be attributed to increased solvent penetration and improved mass transfer kinetics, thereby facilitating the release of a greater quantity of triterpenoid compounds from the plant matrix. Nevertheless, excessively high extraction temperatures may have induced thermal degradation of the targeted triterpenoids, culminating in the observed decrease in TTY at elevated temperatures [29]. Thus, the optimal extraction temperature was considered to be 60 °C.

3.1.5. Effect of the liquid-to-solid ratio on the TTY

The impact of the liquid-to-solid ratio on TTY is illustrated in Fig. 1E. The TTY substantially increased from 20.65 ± 0.46 to 34.41 ± 0.75 mg/g as the liquid-to-solid ratio increased from 10 to 25 mL/g, which was attributed to the increased concentration gradient, which served as the driving force for TTY mass transfer. However, further increases in the liquid-to-solid ratio did not yield significant changes in TTY. A similar trend was also reported for the UAE of triterpenoids from *Jatropha curcas* leaves [8]. Moreover, owing to the potential increase in recovery costs associated with a higher liquid-to-solid ratio, the optimal ratio was determined to be 25 mL/g.

3.1.6. Effect of the number of extraction cycles on the TTY

The impact of the number of extraction cycles on TTY is illustrated in Fig. 1F. As the number of extraction cycles increased from 1 to 2, TTY significantly increased from 21.52 ± 0.76 to 29.75 ± 0.73 mg/g, whereas further increasing the number of extraction cycles did not result in a substantial increase in TTY. Considering both operational costs and efficiency, the optimal number of extraction cycles was determined to be 2.

3.2. Optimization of the UAE parameters via RSM

3.2.1. Model fitting and statistical analysis

The data obtained under various conditions in the BBD are presented in Table 1, which shows that the TTY ranged from 25.34 to 36.40 mg/g. Multiple regression analysis was then conducted to examine the experimental data, offering valuable insights for parameter optimization and facilitating a comprehensive understanding of the intricate relationships between the independent and dependent variables. The resulting model employed a quadratic polynomial equation, as represented by Eq. (2).

$$Y = 35.85 - 1.79X_1 + 1.80X_2 - 1.60X_3 - 1.19X_4 - 2.01X_1X_2 - 0.8625X_1X_3 + 1.25X_1X_4 - 3.64X_2X_3 + 2.38X_2X_4 - 3.06X_3X_4 - 3.04X_1^2 - 3.82X_2^2 - 2.31X_3^2 - 0.5564X_4^2 \quad (2)$$

The regression model was assessed for its fitness and adequacy through ANOVA, with the results summarized in Table 2. The *F* value (34.39) and *p* value (<0.0001) of the regression model suggested its high significance, demonstrating the ability to adequately describe the relationships between the independent variables and the response. The "lack of fit" was deemed statistically insignificant relative to the pure error, as evidenced by the *F* value (2.08) and *p* value (0.2506), suggesting that there was a 13.35 % probability that a "lack of fit" *F* value

Table 1
BBD and corresponding response values.

Run	X_1 (%)	X_2 (W)	X_3 (min)	X_4 (°C)	Y (mg/g)
1	75	400	40	60	35.89
2	95	300	40	60	26.24
3	85	350	40	60	36.31
4	75	350	30	60	32.52
5	85	350	30	50	33.12
6	85	400	30	60	36.27
7	75	300	40	60	27.90
8	75	350	40	70	30.87
9	85	300	40	50	33.25
10	85	350	40	60	36.39
11	75	350	50	60	31.60
12	85	350	50	50	35.91
13	95	350	50	60	27.32
14	75	350	40	50	35.45
15	85	350	50	70	26.87
16	85	350	40	60	36.36
17	85	350	40	60	34.98
18	85	400	50	60	25.34
19	95	350	30	60	31.69
20	85	350	30	70	36.33
21	95	350	40	50	30.43
22	85	400	40	50	32.42
23	85	300	50	60	29.75
24	85	400	40	70	35.02
25	85	350	40	60	35.22
26	95	350	40	70	30.85
27	85	300	40	70	26.33
28	85	300	30	60	26.11
29	95	400	40	60	26.20

Note: X_1 – EtOH concentration; X_2 – ultrasonic power; X_3 – extraction time; X_4 – extraction temperature; Y – total triterpenoids yield.

Table 2
ANOVA for quadratic model.

Source	Sum of Squares	df	Mean Square	F-value	p-value
Model	408.46	14	29.18	34.39	< 0.0001
X_1	38.52	1	38.52	45.41	< 0.0001
X_2	38.74	1	38.74	45.66	< 0.0001
X_3	30.88	1	30.88	36.40	< 0.0001
X_4	17.06	1	17.06	20.11	0.0005
X_1X_2	16.12	1	16.12	19.00	0.0007
X_1X_3	2.98	1	2.98	3.51	0.0821
X_1X_4	6.25	1	6.25	7.37	0.0168
X_2X_3	53.07	1	53.07	62.56	< 0.0001
X_2X_4	22.66	1	22.66	26.71	0.0001
X_3X_4	37.52	1	37.52	44.22	< 0.0001
X_1^2	60.05	1	60.05	70.78	< 0.0001
X_2^2	94.79	1	94.79	111.73	< 0.0001
X_3^2	34.58	1	34.58	40.76	< 0.0001
X_4^2	2.01	1	2.01	2.37	0.1462
Residual	11.88	14	0.8484		
Lack of fit	9.96	10	0.9960	2.08	0.2506
Pure error	1.92	4	0.4793		
Cor total	420.34	28			

Note: X_1 – EtOH concentration; X_2 – ultrasonic power; X_3 – extraction time; X_4 – extraction temperature; df – degrees of freedom.

this large could occur be large due to the noise. The predicted R^2 of 0.8564 was in reasonable agreement with the adjusted R^2 of 0.9435 (with a difference of less than 0.2), confirming the consistency between the predicted and experimental values [30]. The data exhibited excellent fit and reproducibility as a result of the relatively low coefficient of variability (C.V.% = 2.89) [28]. Additionally, X_1, X_2, X_3, X_4, X_1^2, X_2^2, X_3^2, X_1X_2, X_1X_4, X_2X_3, X_2X_4, and X_3X_4 demonstrated statistically significant impacts on the TTY ($p < 0.05$).

3.2.2. Response surface analysis and numerical optimization

Three-dimensional (3D) surface plots and two-dimensional (2D) contour plots provide a visually engaging depiction of how two independent variables interact and influence the dependent variable, facilitating a comprehensive analysis while controlling all other factors at a zero level. RSM analysis offers valuable insights, enabling the identification of the optimal levels of each variable necessary to achieve the maximum response value [31]. As indicated in Fig. 2, within the scope of the study, TTY demonstrated significant sensitivity to X_1, X_2, X_3, and X_4 ($p < 0.05$), in line with the ANOVA findings. As seen from the steep 3D surface and noncircular 2D contour plots, the interactions X_1X_2, X_1X_4, X_2X_3, X_2X_4 and X_3X_4 also had a significant effect on TTY ($p < 0.05$), indicating strong interdependencies between the independent variables. However, it could be inferred from the relatively gentle 3D surface and nearly circular 2D plot that the interaction effect of X_1X_3 on TTY was not significant ($p > 0.05$), which was consistent with the results of the ANOVA. The optimal combination of four variables for achieving the maximum TTY through the numerical desirability function was determined as follows: EtOH concentration 93.37 %; ultrasonic power 390.21 W; extraction time 30 min; and extraction temperature 70 °C.

3.2.3. Model validation

Given the requirements for operational maneuverability and control precision, the efficacy of the predictive model was evaluated under modified process parameters, including an EtOH concentration of 93 %, an ultrasonic power of 390 W, an extraction time of 30 min, an extraction temperature of 70 °C, a liquid-to-solid ratio of 25 mL/g, and 2 extraction cycles. The validation experiment was repeated three times, yielding a TTY of 36.77 ± 0.40 mg/g, which aligned well with the predicted value of 36.90 mg/g. These results offered compelling support for the practical utility of the prediction model advanced in this study.

Additionally, the TTY obtained from traditional heat reflux extraction was 24.13 ± 0.63 mg/g, highlighting the effectiveness of UAE technology. This increase can be attributed to ultrasonic cavitation, which generates microbubbles that collapse violently, creating localized high temperatures and pressures. This process disrupts plant cell walls and enhances solvent penetration. Furthermore, the turbulence induced by ultrasonic waves improves mixing and facilitates solvent distribution, further enhancing extraction efficiency.

3.3. Enrichment of total triterpenoids

The elution profile depicted in Fig. 3 revealed that H_2O, 30 % EtOH, and 60 % EtOH exhibited limited efficacy in the elution of triterpenoids, implying their potential effectiveness for the elimination of highly polar impurities, such as phenolic compounds. In contrast, 90 % EtOH demonstrated superior elution usefulness for triterpenoids, indicating its suitability for targeted compounds recovery. The fraction corresponding to the shaded region in Fig. 3 was collected, concentrated under reduced pressure, and subjected to freeze-drying to obtain the TRF. Quantitative analysis of the TRF revealed a satisfactory total triterpenoids recovery of 81.71 ± 0.90 %, with the purity significantly increasing from 18.46 ± 0.78 % to 73.27 ± 0.84 %, highlighting the effectiveness of the employed chromatographic separation strategy.

3.4. UPLC–ESI-QTOF-MS/MS analysis

A total of thirteen compounds, including eight pentacyclic triterpenoid acids, four chain fatty acids, and one alicyclic acid, were unambiguously confirmed or tentatively identified in TRF via UPLC–QTOF-MS/MS (Table 3). Fig. 4 displays the overlapped EIC peaks of these compounds, and their chemical structures are shown in Fig. S1. Compound 1, with an $[M-H]^-$ ion at m/z 191.0571, produced a fragment ion at m/z 85.0296 owing to the loss of 1,2,3-butanetriol, and it was identified as quinic acid [32]. Compound 2, with an $[M-H]^-$ ion at m/z 487.3425, produced fragment ions at m/z 469.3322 and 423.3253 and was identified as tormentic acid, as reported in the literature [33]. Compounds 3 and 4, with $[M-H]^-$ ions at m/z 471.3469 and 471.3470, respectively, produced the fragment ions at m/z 453.3378 and 453.3368

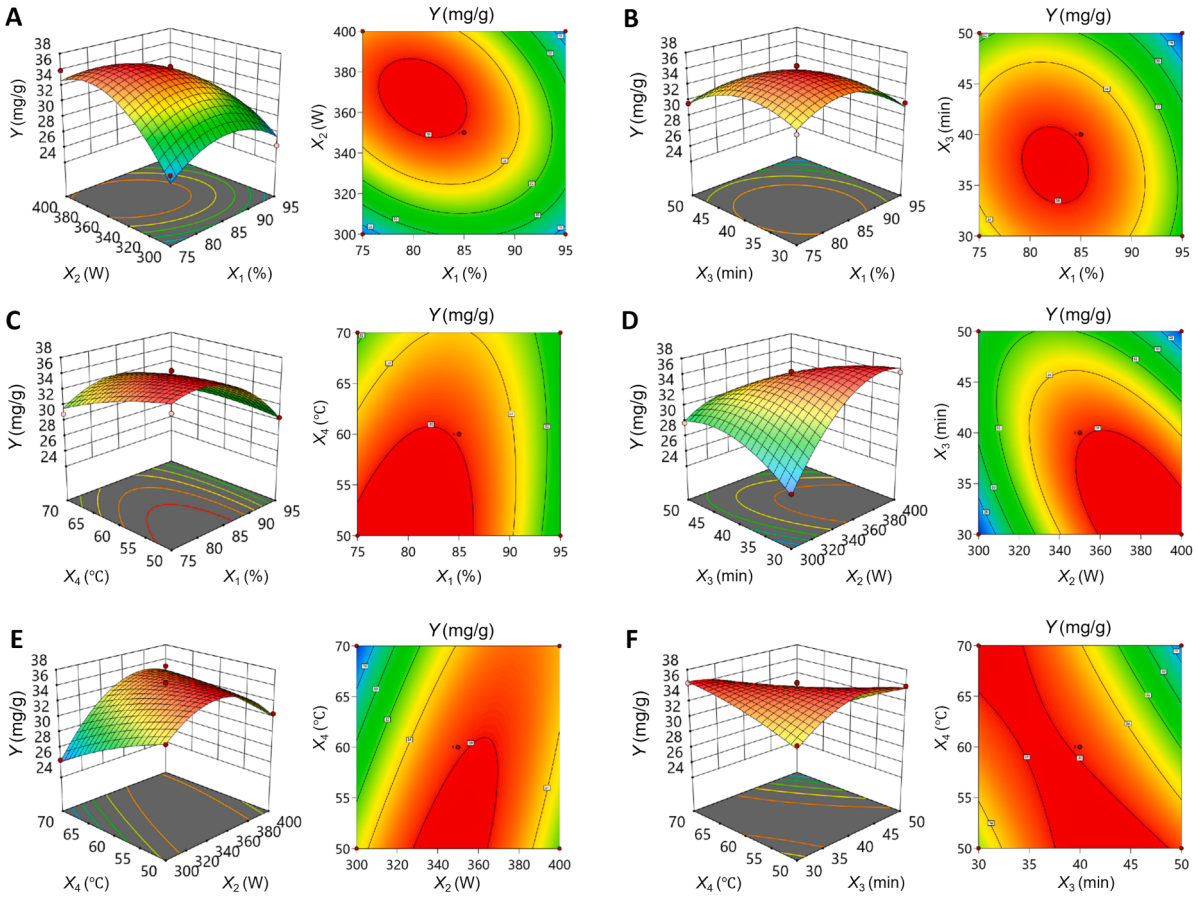

Fig. 2. Response surface plots and contour plots for the interaction between different factors affecting TTY. (A) X_1 and X_2; (B) X_1 and X_3 (C) X_1 and X_4; (D) X_2 and X_3; (E) X_2 and X_4; (F) X_3 and X_4.

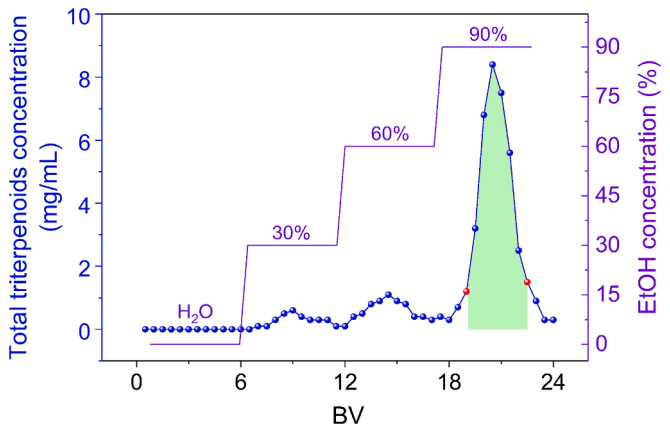

Fig. 3. Gradient elution curve.

([M−H−H_2O]$^-$) and were identified as pomolic acid and maslinic acid by comparing their UPLC retention times (t_R) and mass spectrometry data with reference standards. Compound 5 was identified as 3-*O*-acetylpomolic acid, with fragment ions at *m/z* 495.3474 [M−H−H_2O]$^-$ and 453.1395 [M−H−H_2O−C_2H_2O]$^-$, as reported in the literature [34]. Compounds 7, 9, and 10 were identified as isomers with the chemical formula $C_{30}H_{48}O_3$. The chemical structure of compound 7 exhibited stability, and no MS/MS ions were detected under the given mass spectrometry conditions, identifying it as betulinic acid by comparing its t_R and mass spectrometry data with a reference standard. Compounds 9 and 10 produced fragment ions at *m/z* 407.3297 and 407.3320 [M−H−H_2O−CH_2O]$^-$, and were identified as oleanolic acid and ursolic acid, respectively, by comparing their t_R and mass spectrometry data with reference standards. Compound 8, with an [M−H]$^-$ ion at *m/z* 277.2185 and a fragment ion at *m/z* 59.0138, was tentatively identified as γ-linolenic acid, as reported in the literature [32]. Compound 12, with an [M−H]$^-$ ion at *m/z* 497.3642, was identified as 3-*O*-acetylursolic acid by comparing the reference standard. Compounds 6, 11, and 13 were identified as chain fatty acids, namely, 16-hydroxyhexadecanoic acid, palmitic acid, and stearic acid, respectively, by comparing their t_R and mass spectrometry data to reference standards.

3.5. HPLC-QQQ-MS quantitative analysis

3.5.1. Establishment and verification of the quantitative method

The optimization of mobile phase composition, elution program, and column type was conducted to achieve desirable chromatographic resolution for five triterpenoid compounds. The inherent structural stability of triterpenoids prevents the generation of fragment ions, even at high collision energies. Therefore, the SIM mode was utilized for the quantification of triterpenoid compounds. Better ionization signals of the five triterpenoid compounds were observed in negative mode. This strategic approach involved selecting the [M−H]$^-$ ion at *m/z* 455.4 for detecting betulinic acid, oleanolic acid, and ursolic acid. Similarly, the [M−H]$^-$ ion at *m/z* 471.3 was used for the detection of pomolic acid and maslinic acid. As shown in Table 4, the standard curves for these analytes demonstrated good linearity, with R^2 values greater than 0.99 across the tested concentration ranges. The RSDs of the intraday and interday peak areas of the five analytes were all less than 5 %, indicating that the method possessed good precision. The recovery rates of theses analytes ranged between 97.94 ± 2.17 % and 102.54 ± 1.29 %,

Table 3
Thirteen compounds in TRF were characterized using UPLC–QTOF-MS/MS.

Peak No.	t_R (min)	Identification	$[M-H]^-$ (*m/z*)	Error (ppm)	Molecular formula	MS/MS (*m/z*)
1	0.631	Quinic acid	191.0571	5.23	$C_7H_{12}O_6$	85.0296
2	1.620	Tormentic acid	487.3425	−0.82	$C_{30}H_{48}O_5$	469.3322, 423.3253
3#	3.395	Pomolic acid	471.3469	−2.33	$C_{30}H_{48}O_4$	453.3378, 407.3340, 451.3223
4#	3.828	Maslinic acid	471.3470	−2.12	$C_{30}H_{48}O_4$	453.3368, 407.3320
5	8.099	3-*O*-Acetylpomolic acid	513.3584	−0.19	$C_{32}H_{50}O_5$	495.3474, 453.1395
6#	8.186	16-Hydroxyhexadecanoic acid	271.2281	1.11	$C_{16}H_{32}O_3$	–
7#	8.519	Betulinic acid	455.3530	−0.22	$C_{30}H_{48}O_3$	–
8	8.563	γ-Linolenic acid	277.2185	4.33	$C_{18}H_{30}O_2$	59.0138
9#	9.279	Oleanolic acid	455.3533	0.44	$C_{30}H_{48}O_3$	407.3297
10#	9.615	Ursolic acid	455.3524	−1.54	$C_{30}H_{48}O_3$	407.3320
11#	13.159	Palmitic acid	255.2331	0.39	$C_{16}H_{32}O_2$	–
12#	14.440	3-*O*-Acetylursolic acid	497.3642	1.21	$C_{32}H_{50}O_4$	–
13#	15.814	Stearic acid	283.2641	−0.71	$C_{18}H_{36}O_2$	–

Note: t_R – retention time; # – identification through comparison with standards.

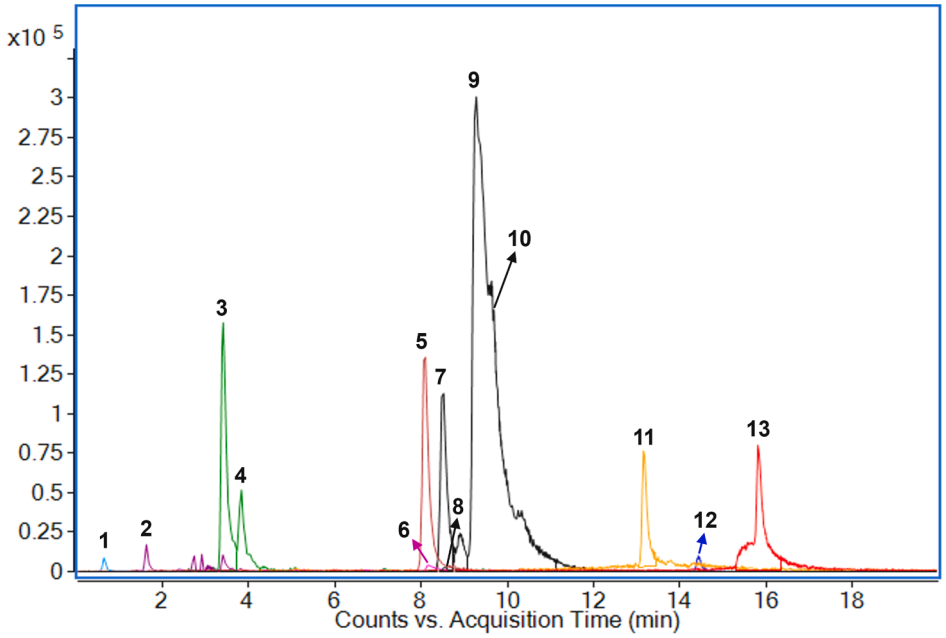

Fig. 4. The overlapped EIC peaks of identified compounds.

Table 4
Method validation for simultaneous quantification of five triterpenoid compounds and their contents.

Compounds	t_R (min)	Regression equation	R^2	Linear range (μg/mL)	LOD (ng/mL)	LOQ (ng/mL)	Precision (RSD, %) Intraday	Interday	Recovery (%)	Content (%) BE	AE
Pomolic acid	6.46	$y = 298547x - 1267$	0.9976	0.05 – 1.0	1.24	4.39	2.65	3.86	98.75 ± 2.56	0.63 ± 0.05	3.05 ± 0.16
Maslinic acid	7.87	$y = 587231x - 9280$	0.9984	0.05 – 1.0	0.15	0.56	3.22	4.71	102.54 ± 1.29	0.18 ± 0.03	1.14 ± 0.07
Betulinic acid	10.81	$y = 1224896x - 21975$	0.9990	0.05 – 1.0	0.08	0.28	1.91	1.83	97.94 ± 2.17	0.29 ± 0.03	1.92 ± 0.11
Oleanolic acid	11.32	$y = 439146x - 1064$	0.9992	0.2 – 10.0	0.27	0.90	3.56	4.49	98.65 ± 3.70	6.14 ± 0.16	28.21 ± 0.62
Ursolic acid	11.87	$y = 392528x + 4627$	0.9991	0.2 – 10.0	0.32	1.25	2.15	4.80	99.92 ± 2.61	5.38 ± 0.21	26.53 ± 0.49

Note: t_R – retention time; LOD – limit of detection; LOQ – limit of quantification; AE – after enrichment; BE – before enrichment.

reflecting excellent accuracy.

3.5.2. *Quantification of five triterpenoid compounds*

The developed HPLC-QQQ-MS method enabled the simultaneous quantification of five pentacyclic triterpenoid compounds (pomolic acid, maslinic acid, betulinic acid, oleanolic acid, and ursolic acid). The SIM signals for the five triterpenoid standards are displayed in Fig. 5A, while Fig. 5B and 5C illustrate the SIM signals for these compounds in the TRF. As shown in Table 4, after enrichment via X-5 resin column chromatography, the contents of five triterpenoid compounds increased 4- to 7-fold, with betulinic acid experiencing the greatest increase by a factor of 6.62, followed by maslinic acid, with a 6.33-fold increase. The overall content of these compounds increased nearly 5-fold after enrichment. The results illustrated that the adsorptive enrichment

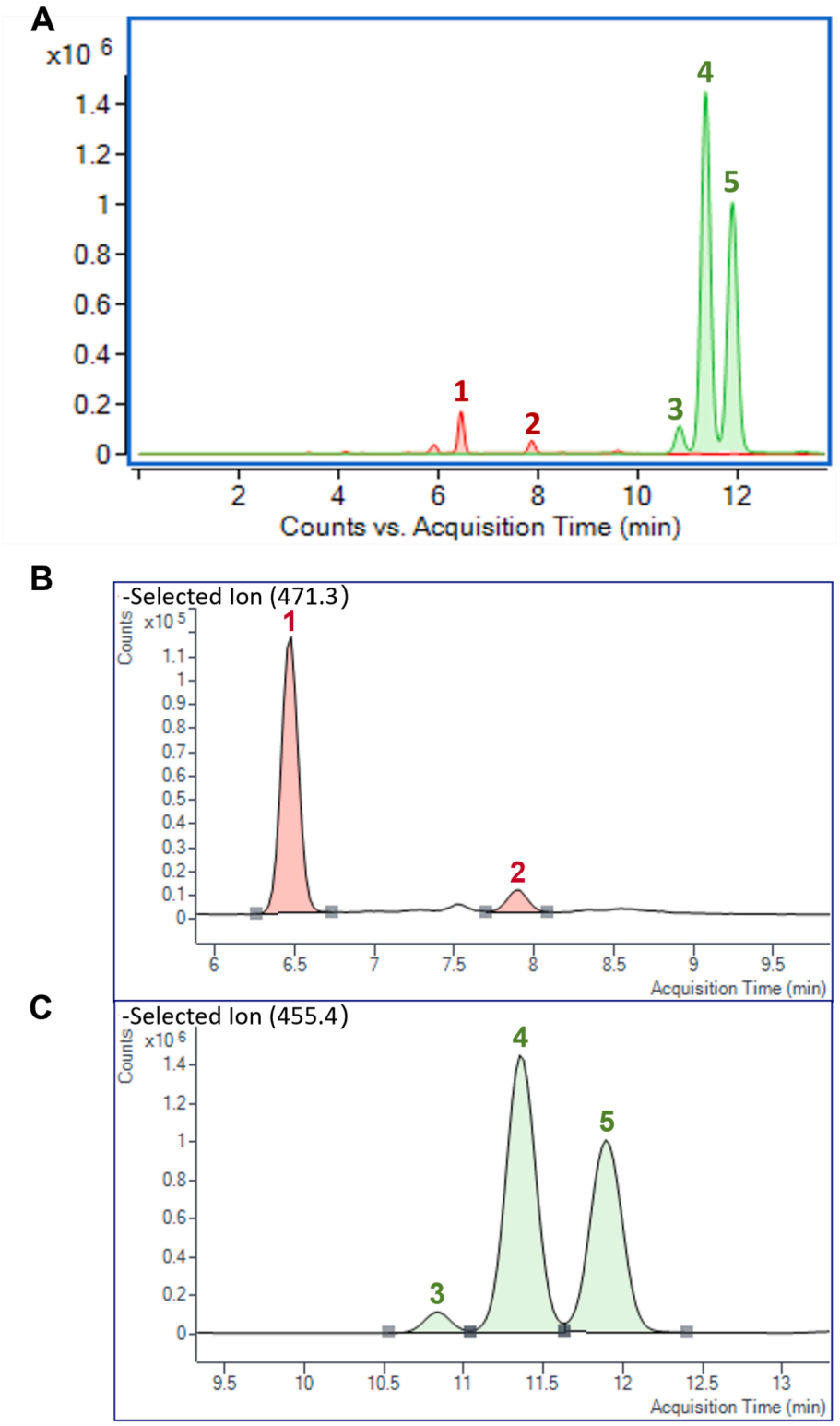

Fig. 5. (A) The SIM signals for the five triterpenoid standards; (B) The SIM signals for pomolic acid (peak 1) and maslinic acid (peak 2) in TRF; (C) The SIM signals for betulinic acid (peak 3), oleanolic acid (peak 4), and ursolic acid (peak 5) in TRF.

method established in this work was efficient in enriching triterpenoids from *C. speciosa* leaves.

3.6. Protection of TRF against ulcerative colitis in mice

The therapeutic efficacy of TRF in treating ulcerative colitis in mice was evaluated, with the ulcerative colitis mouse model and drug administration protocol shown in Fig. 6A. As depicted in Fig. 6B, the body weight gradually increased over time in the normal group (106.24 ± 2.32 %). In contrast, the model group exhibited significant body weight loss (84.35 ± 3.41 %), whereas TRF noticeably alleviated the weight loss trend in ulcerative colitis mice. A significant difference was observed in the DAI scores depicted in Fig. 6C, with the model group showing higher scores than the other groups from days 4 to 9; however,

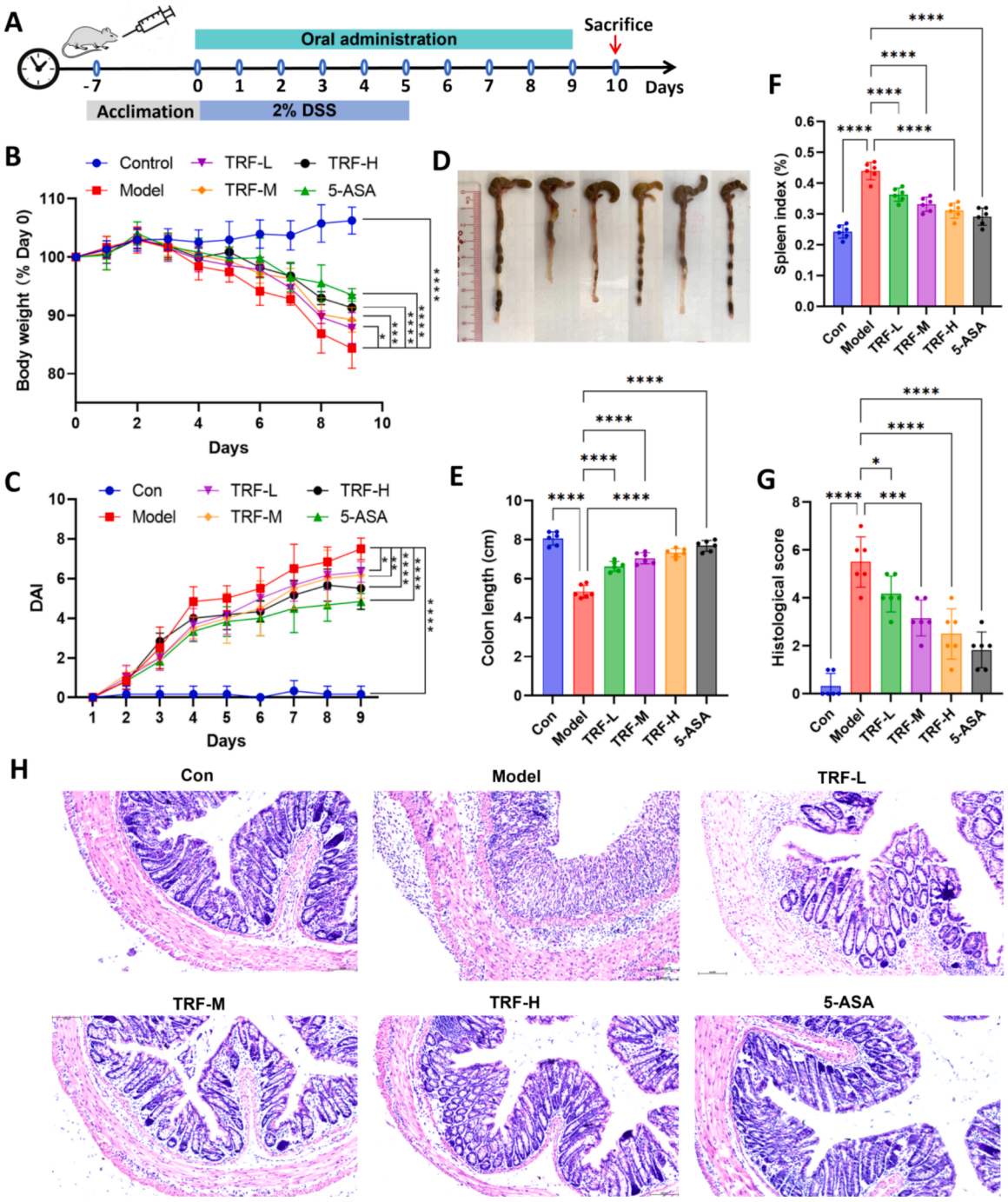

Fig. 6. Protection of TRF against ulcerative colitis in mice. (A) Experimental design diagram; (B) Daily bodyweight changes of mice; (C) DAI scores of mice in each group; (D) Representative colon tissue images of mice in each group; (E) Histogram of colon length of mice in each group; (F) Histogram of spleen index of mice in each group; (G) Histological scores determined from H&E-stained colons of mice in each group; (H) Representative H&E staining images of colon tissues from mice in each group. $^{*}p < 0.05$, $^{**}p < 0.01$, $^{***}p < 0.001$, $^{****}p < 0.0001$ compared to the model group.

the TRF treatments significantly reduced the DAI scores, indicating a promising therapeutic effect. After the mice were euthanized on the 10th day, their colon and spleen tissues were also analyzed. As shown in Fig. 6D and E, the colon length of the drug intervention groups was notably longer than that of the model group, indicating that TRF had a beneficial inhibitory effect on the characteristic colon shortening typically observed in DSS-induced ulcerative colitis. Moreover, the spleen index of each group was detected. As shown in Fig. 6F, the spleen index of the model group was significantly greater than that of the normal group, indicating that DSS treatment caused severe inflammation, whereas TRF treatment markedly reduced the spleen index, indicating a great alleviation of inflammation. Fig. 6G presents the histological scores derived from the results of H&E staining (Fig. 6H). Compared with normal group, the colonic tissues of DSS group exhibited inflammation characterized by colonic epithelial damage, infiltration of various inflammatory cells, and reduced numbers of mucin-secreting goblet cells. The crypt integrity in the TRF treatment groups was superior to that in the DSS group, suggesting that TRF could improve symptoms of colonic inflammation. It could be inferred that the therapeutic effectiveness of TRF in treating ulcerative colitis was primarily

attributed to its principal bioactive components, oleanolic acid, and ursolic acid. Oleanolic acid has been demonstrated to ameliorate DSS-induced ulcerative colitis in mouse model by restoring the dysregulated balance between Th17 and Treg cells, as well as by inhibiting the NF-κB signaling pathway [35]. Complementarily, ursolic acid has been shown to modulate the intestinal microbiota composition and suppress inflammatory cell infiltration, thereby effectively preventing the development of ulcerative colitis in mice [36].

4. Conclusions

The present work is the first to recover triterpenoid compounds from *C. speciosa* leaves via UAE coupled with adsorptive enrichment, demonstrating the effectiveness and feasibility of this green strategy. The optimal UAE parameters were meticulously established through RSM, culminating in a commendable yield of total triterpenoids of 36.77 ± 0.40 mg/g. After one-step enrichment via X-5 resin column chromatography, the content of total triterpenoids in the *C. speciosa* leaves extract increased from 18.46 ± 0.78 % to 73.27 ± 0.84 %. Thirteen components in TRF, including eight pentacyclic triterpenoid acids, four chain fatty acids, and one alicyclic acid, were identified through UPLC–QTOF-MS/MS. Five major triterpenoid compounds were quantified simultaneously using the developed HPLC-QQQ-MS method, providing a reliable approach for the quality control of TRF. Furthermore, a pharmacological study showed that TRF was able to effectively protect against DSS-induced ulcerative colitis in mice. In summary, this study will contribute to improving the utilization of *C. speciosa* leaves, thereby bringing additional medicinal value.

CRediT authorship contribution statement

Mengyang Hou: Writing – original draft, Methodology, Investigation, Data curation, Conceptualization. **Jingchun Shi:** Software, Methodology, Investigation, Data curation. **Chengyuan Lin:** Project administration, Formal analysis, Conceptualization. **Lin Zhu:** Writing – review & editing, Validation, Funding acquisition. **Zhaoxiang Bian:** Writing – review & editing, Resources, Project administration, Funding acquisition.

Declaration of Competing Interest

The authors declare that they have no known competing financial interests or personal relationships that could have appeared to influence the work reported in this paper.

Acknowledgments

This work was funded by the Health@InnoHK Initiative Fund of the Hong Kong Special Administrative Region Government (ITC RC/IHK/4/7) and the Key-Area Research and Development Program of Guangdong Province (2020B1111110003).

Appendix A. Supplementary data

Supplementary data to this article can be found online at https://doi.org/10.1016/j.ultsonch.2024.107136.

References

[1] R. Xu, M. Kuang, N. Li, Phytochemistry and pharmacology of plants in the genus *Chaenomeles*, Arch. Pharm. Res. 46 (2023) 825–854, https://doi.org/10.1007/s12272-023-01475-w.

[2] R. Zhang, S. Li, Z. Zhu, J. He, Recent advances in valorization of *Chaenomeles* fruit: A review of botanical profile, phytochemistry, advanced extraction technologies and bioactivities, Trends Food Sci. Tech. 91 (2019) 467–482, https://doi.org/10.1016/j.tifs.2019.07.012.

[3] M. Hou, C. Lin, Y. Ma, J. Shi, J. Liu, L. Zhu, Z. Bian, One-step enrichment of phenolics from *Chaenomeles speciosa* (Sweet) Nakai fruit using macroporous resin: Adsorption/desorption characteristics, process optimization and UPLC-QqQ-MS/MS-based quantification, Food Chem. 439 (2024) 138085, https://doi.org/10.1016/j.foodchem.2023.138085.

[4] S.Y. Zhang, L.Y. Han, H. Zhang, H.L. Xin, *Chaenomeles speciosa*: A review of chemistry and pharmacology, Biomed. Rep. 2 (2014) 12–18, https://doi.org/10.3892/br.2013.193.

[5] I.P. Turkiewicz, A. Wojdyło, K. Tkacz, P. Nowicka, UPLC/ESI-Q-TOF-MS analysis of (poly) phenols, tocols and amino acids in *Chaenomeles* leaves versus *in vitro* anti-enzyme activities, Ind. Crop Prod. 181 (2022) 114829, https://doi.org/10.1016/j.indcrop.2022.114829.

[6] C. Chen, Q. Ai, A. Shi, N. Wang, L. Wang, Y. Wei, Oleanolic acid and ursolic acid: Therapeutic potential in neurodegenerative diseases, neuropsychiatric diseases and other brain disorders, Nutr. Neurosci. 26 (2023) 414–428, https://doi.org/10.1080/1028415X.2022.2051957.

[7] A.K. Jha, N. Sit, Extraction of bioactive compounds from plant materials using combination of various novel methods: A review, Trends Food Sci. Tech. 119 (2022) 579–591, https://doi.org/10.1016/j.tifs.2021.11.019.

[8] L. Wei, W. Zhang, L. Yin, F. Yan, Y. Xu, F. Chen, Extraction optimization of total triterpenoids from *Jatropha curcas* leaves using response surface methodology and evaluations of their antimicrobial and antioxidant capacities, Electron. J. Biotechn. 18 (2015) 88–95, https://doi.org/10.1016/j.ejbt.2014.12.005.

[9] F. Chemat, N. Rombaut, A.G. Sicaire, A. Meullemiestre, A.S. Fabiano-Tixier, M. Abert-Vian, Ultrasound assisted extraction of food and natural products. Mechanisms, techniques, combinations, protocols and applications. A review, Ultrason. Sonochem. 34 (2017) 540–560, https://doi.org/10.1016/j.ultsonch.2016.06.035.

[10] M.M. Rahman, B.P. Lamsal, Ultrasound-assisted extraction and modification of plant-based proteins: Impact on physicochemical, functional, and nutritional properties, Compr. Rev. Food Sci. f. 20 (2021) 1457–1480, https://doi.org/10.1111/1541-4337.12709.

[11] Y. Yang, Q. Liang, B. Zhang, J. Zhang, L. Fan, J. Kang, Y. Lin, Y. Huang, T.C. Tan, L. H. Ho, Adsorption and desorption characteristics of flavonoids from white tea using macroporous adsorption resin, J. Chromatogr. A 1715 (2024) 464621, https://doi.org/10.1016/j.chroma.2023.464621.

[12] Y. Xue, F. Wang, C. Zhou, Optimization of ultrasonic extraction of triterpenes from loquat peel and pulp and determination of antioxidant activity and triterpenoid components, Foods 11 (2022) 2563, https://doi.org/10.3390/foods11172563.

[13] Y. Fu, Y. Zhang, R. Zhang, Purification and antioxidant properties of triterpenic acids from blackened jujube (*Ziziphus jujuba* Mill.) by macroporous resins, Food Sci. Nutr. 9 (2021) 5070–5082, https://doi.org/10.1002/fsn3.2464.

[14] M.F. Guo, J. Zhou, H.H. Zhang, P. Zhong, J.D. Xu, S.S. Zhou, F. Long, H. Zhu, Q. Mao, S.L. Li, UPLC-QTOF-MS/MS assisted UPLC-TQ-MS/MS strategy to comparatively investigate the rat pharmacokinetics of N-acetyldopamine oligomers derived from Cicadae Periostracum, J. Chromatogr. B 1226 (2023) 123806, https://doi.org/10.1016/j.jchromb.2023.123806.

[15] U. Boesl, Time-of-flight mass spectrometry: introduction to the basics, Mass Spectrom Rev. 36 (2017) 86–109, https://doi.org/10.1002/mas.21520.

[16] B. Yang, H. Li, Q.F. Ruan, Y.Y. Xue, D. Cao, X.H. Zhou, S.Q. Jiang, T. Yi, J. Jin, Z. X. Zhao, A facile and selective approach to the qualitative and quantitative analysis of triterpenoids and phenylpropanoids by UPLC/Q-TOF-MS/MS for the quality control of *Ilex rotunda*, J. Pharmaceut. Biomeds. 157 (2018) 44–58, https://doi.org/10.1016/j.jpba.2018.05.002.

[17] M. Dai, S. Li, Q. Shi, X. Xiang, Y. Jin, S. Wei, L. Zhang, M. Yang, C. Song, R. Huang, S. Jin, Changes in triterpenes in alismatis rhizoma after processing based on targeted metabolomics using UHPLC-QTOF-MS/MS, Molecules 27 (2021) 185, https://doi.org/10.3390/molecules27010185.

[18] F. Zheng, X. Zhao, Z. Zeng, L. Wang, W. Lv, Q. Wang, G. Xu, Development of a plasma pseudotargeted metabolomics method based on ultra-high-performance liquid chromatography–mass spectrometry, Nat. Protoc. 15 (2020) 2519–2537, https://doi.org/10.1038/s41596-020-0341-5.

[19] P.T. Santana, S.L.B. Rosas, B.E. Ribeiro, Y. Marinho, H.S. de Souza, Dysbiosis in inflammatory bowel disease: pathogenic role and potential therapeutic targets, Int. J. Mol. Sci. 23 (2022) 3464, https://doi.org/10.3390/ijms23073464.

[20] R. Han, L. Wang, Z. Zhao, L. You, S. Pedisić, V. Kulikouskaya, Z. Lin, Polysaccharide from *Gracilaria Lemaneiformis* prevents colitis in Balb/c mice via enhancing intestinal barrier function and attenuating intestinal inflammation, Food Hydrocolloid. 109 (2020) 106048, https://doi.org/10.1016/j.foodhyd.2020.106048.

[21] J.S. Shin, E.J. Cho, H.E. Choi, J.H. Seo, H.J. An, H.J. Park, Y.W. Cho, K.T. Lee, Anti-inflammatory effect of a standardized triterpenoid-rich fraction isolated from *Rubus coreanus* on dextran sodium sulfate-induced acute colitis in mice and LPS-induced macrophages, J. Ethnopharmacol. 158 (2014) 291–300, https://doi.org/10.1016/j.jep.2014.10.044.

[22] J. Chun, C. Lee, S.W. Hwang, J.P. Im, J.S. Kim, Ursolic acid inhibits nuclear factor-κB signaling in intestinal epithelial cells and macrophages, and attenuates experimental colitis in mice, Life Sci. 110 (2014) 23–34, https://doi.org/10.1016/j.lfs.2014.06.018.

[23] T. Nakagawa, Q. Zhu, S. Tamrakar, Y. Amen, Y. Mori, H. Suhara, S. Kaneko, H. Kawashima, K. Okuzono, Y. Inoue, K. Ohnuki, K. Shimizu, K., Changes in content of triterpenoids and polysaccharides in *Ganoderma lingzhi* at different growth stages, J. Nat. Med-Tokyo 72 (2018) 734–744, https://doi.org/10.1007/s11418-018-1213-y.

[24] Y.H. Li, R. Adam, J.F. Colombel, Z.X. Bian, A characterization of pro-inflammatory cytokines in dextran sulfate sodium-induced chronic relapsing colitis mice model, Int. Immunopharmacol. 60 (2018) 194–201, https://doi.org/10.1016/j.intimp.2018.05.001.

[25] Y. Lee, K. Sugihara, M.G. Gillilland III, S. Jon, N. Kamada, J.J. Moon, Hyaluronic acid–bilirubin nanomedicine for targeted modulation of dysregulated intestinal barrier, microbiome and immune responses in colitis, Nat. Mater. 19 (2020) 118–126, https://doi.org/10.1038/s41563-019-0462-9.

[26] L. Shen, S. Pang, M. Zhong, Y. Sun, A. Qayum, Y. Liu, A. Rashid, B. Xu, Q. Liang, H. Ma, X. Ren, A comprehensive review of ultrasonic assisted extraction (UAE) for bioactive components: Principles, advantages, equipment, and combined technologies, Ultrason. Sonochem. 101 (2023) 106646, https://doi.org/10.1016/j.ultsonch.2023.106646.

[27] F. Tie, Q. Dong, X. Zhu, L. Ren, Z. Liu, Z. Wang, H. Wang, N. Hu, Optimized extraction, enrichment, identification and hypoglycemic effects of triterpenoid acids from *Hippophae rhamnoides* L pomace, Food Chem. 457 (2024) 140143, https://doi.org/10.1016/j.foodchem.2024.140143.

[28] Y. Sun, J. Lu, J. Li, P. Li, M. Zhao, G. Xia, Optimization of ultrasonic-assisted extraction of polyphenol from Areca nut (*Areca catechu* L.) seeds using response surface methodology and its effects on osteogenic activity, Ultrason. Sonochem. 98 (2023) 106511, https://doi.org/10.1016/j.ultsonch.2023.106646.

[29] L. Guo, X. Li, J. Zhang, X. Sun, Y. Li, H. Kan, Optimization of extraction and macroporous resin purification processes of total triterpenoid from *Boletus edulis* Bull.: Fr, J. Food Process. Pres. 45 (2021) e15292.

[30] C. Li, C. Zhao, Y. Ma, W. Chen, Y. Zheng, X. Zhi, G. Peng, Optimization of ultrasonic-assisted ultrafiltration process for removing bacterial endotoxin from diammonium glycyrrhizinate using response surface methodology, Ultrason. Sonochem. 68 (2020) 105215, https://doi.org/10.1016/j.ultsonch.2020.105215.

[31] M. Hou, W. Hu, A. Wang, Z. Xiu, Y. Shi, K. Hao, X. Sun, D. Cao, R. Lu, J. Sun, Ultrasound-assisted extraction of total flavonoids from *Pteris cretica* L.: process optimization, HPLC analysis, and evaluation of antioxidant activity, Antioxidants 8 (2019) 425, https://doi.org/10.3390/antiox8100425.

[32] W. Tao, C. Zhao, G. Lin, Q. Wang, Q. Lv, S. Wang, Y. Chen, UPLC-ESI-QTOF-MS/MS analysis of the phytochemical compositions from *Chaenomeles speciosa* (sweet) Nakai fruits, J. Chromatogr. Sci. 61 (2023) 15–31, https://doi.org/10.1093/chromsci/bmac002.

[33] H. Li, W. Yao, Q. Liu, J. Xu, B. Bao, M. Shan, Y. Cao, F. Cheng, A. Ding, L. Zhang, Application of UHPLC-ESI-Q-TOF-MS to identify multiple constituents in processed products of the herbal medicine Ligustri Lucidi Fructus, Molecules 22 (2017) 689, https://doi.org/10.3390/molecules22050689.

[34] M. Sun, H. Zhao, Y. Liu, Y. Ma, Z. Tian, H. Wang, S. Wei, Q. Guo, Z. Gu, H. Jiang, Deciphering the pharmacological mechanisms of Chaenomeles Fructus against rheumatoid arthritis by integrating network pharmacology and experimental validation, Food Sci. Nutr. 10 (2022) 3380–3394, https://doi.org/10.1002/fsn3.2938.

[35] G.D. Kang, S. Lim, D.H. Kim, Oleanolic acid ameliorates dextran sodium sulfate-induced colitis in mice by restoring the balance of Th17/Treg cells and inhibiting NF-κB signaling pathway, Int. Immunopharmacol. 29 (2015) 393–400, https://doi.org/10.1016/j.intimp.2015.10.024.

[36] Q. Sheng, F. Li, G. Chen, J. Li, J. Li, Y. Wang, Y. Lu, Q. Li, M. Li, K. Chai, Ursolic acid regulates intestinal microbiota and inflammatory cell infiltration to prevent ulcerative colitis, J. Immunol. Res. 2021 (2021) 6679316, https://doi.org/10.1155/2021/6679316.